2024 International Conference on Industrial Engineering, Applications and Manufacturing (ICIEAM)

The Fusion-ICP Data Registration Algorithm Using Ortogonal Transformations for 3D Reconstructing of an Archaeological Sites' Models

A. Vokhmintcev[1,2]
[1]*Institute of Information Technology*
Chelyabinsk State University
Chelyabinsk, Russia
[2]*Institute of Digital Economy*
Ugra State University
Khanty-Mansiysk, Russia
vav@csu.ru

A. Mityanina
Institute of Information Technology
Chelyabinsk State University
Chelyabinsk, Russia
nastya.mityanina@gmail.com

M. Romanov[1,2]
[1]*Institute of Information Technology*
Chelyabinsk State University
Chelyabinsk, Russia
[2] *South Ural State University*
Chelyabinsk, Russia
std.romanov.ma@gmail.com

***Abstract*—In this paper a system for the detection and research of archaeological sites using on machine learning methods, mapping methods and geophysics methods is presented. The development of an information system for remote archaeological research allows, on the one hand, to solve the most important problem of archaeological science, related to the preservation of cultural heritage, and on the other hand, to reduce the duration of the archaeological examination procedure conducted before the industrial development of the territory. In this paper the method for registering 3D data based on ICP (Iterative Closest Points) based on fusion of visual and semantic characteristics of an archaeological site for a class of orthogonal transformations was proposed. Computer modeling of the proposed 3d registration method was carried out using a collection of data from archaeological sites of the Bronze Age of the Southern Trans-Urals. When performing computer modeling, methods for solving the variational ICP problem were considered, using various options for minimizing the functional: the point-to-point metric with and without extrapolation, using the point-to-plane metric. A comparative analysis with various options for minimizing the functional was carried out, the results of computer simulation were presented and discussed.**

Keywords—3d registration task, iterative closest points, tacheometric survey result

I. INTRODUCTION

In archeology, decoding of an archaeological site is often carried out on the basis of 3D relief models obtained from different viewing points. So, there is a need to solve the problem of reconstruction of archaeological monuments [1-4]. Nowdays methodologies for 3d relief terrain reconstruction can be subdivided into three group using the modeling purpose factor: geometry modeling (based on polygonal-structured model), semantic modeling, topological modeling [5].

Group 1. Geometric modeling. Among the science papers of the first group, the works of Horna et al. [6] and Lee et al. [7] should be mentioned. Li et al. [8] suggested an efficient 3d reconstruction approach from plans of archeaological sites to based on 3d matching and classification methods. Due to the rapid development of laser scanning sensors, photogrammetric methods and data recording methods have become widespread for visualization of 3d space, while existing methods for solving the problem can be divided into methods for extracting structural elements: least square-based methods [9], normal analysis methods [10], methods based on random sample consensus [11] and methods for spatial decomposition and reconstruction [12]. In the space 3d reconstruction methods the detail information of indoor structure of archaeological site is used to achieve a more robust 3d registration result. For example, in paper [13] method based on a graph cut-based labeling was presented for reconstructing structural elements of indoor space.

Group 2. Semantic Modeling. In case the semantic modeling the main focuses is diricted on semantic labeling, which is associated with taking into account the belonging of the object to the class of the subject area, unlike geometric modeling, which does not take into account the semantic characteristics of the environment. Semantic Modeling show good results for 3d reconstruction of semantically rich. Among the science papers of the second group Conditional random fields based model [14], a patch descriptor using contextual information and Markov random field model [15] should be mentioned.

Most promising concept using fusion depth information (D-I) and features of super-pixels (F-I) is presented [16]. In this concept D-I is used to optimize image segmentation processing and F-I for automatic classification based on the SVM-classifier and RF (random forest). In recent years various CNN (Convolution Neural Network)-based architectures for semantic segmentation and classifications have been suggested to get high-rate semantic characteristics of the environment. [17-19].

Group 3. Topological modeling. The existing methods of the first group can be devided into three subgroups: subdivision method models [20], grid models [21-22], and hybrid models [23-25]. In paper [21] authors use CNN and Bayesian approach to get high-rate data from a grid map for generating a topological map based on a Voronoi diagram. In paper [25] a semantic and topological information was extracted using occupancy grid mapping algorithm and then represented into a semantic node-relation graph.

979-8-3503-9501-3/24/$31.00 ©2024 IEEE

One of the state of the art well solution in class of Geometric modeling is the Iterative Closest Point (ICP) algorithm [26] and its variants [27]. In this paper we suggest originally 3d registration algorithm Fusion ICP (F-ICP), which allows to reconstruct of an archaeological sites in the form of a point cloud for a group of ortogonal transformations based on solving the ICP variational problem in closed form using the point-to-point metric, singular points and semantic characteristics of an archaeological sites.

The F-ICP method improves the quality of work of two key steps of the ICP method: determining the corresponding points between a pair of three-dimensional point clouds and solving the variational problem, differs from the known versions of the ICP method in that:

- it allows you to solve the problem of the dependence of the result of solving the variational problem on the correct choice of initial values;
- allows you to obtain better convergence and accuracy in comparison with other combined versions of the ICP algorithm, which are based on the joint solution of the variational ICP problem and use the fusion of data on the color and depth of the RGB-D frame.

In this work, only large objects inside archaeological sites are considered, such as contours and details of external and internal architectural structures of ancient settlements, religious monuments, sites, burial mounds and ground burial grounds, sanctuaries, megaliths, dolmens and ancient mines.

This article is organized as follows: in the second section, the variational problem of the F-ICP for ortogonal transformations is given, in the third section an accurated fusion ICP algorithm for ortogonal transformation is presented, in the fourth section, the obtained results of computer modeling were presented and discussed.

II. Variational Problem of the F-ICP for Ortogonal Transformations

Consider the variational problem of the F-ICP using a point-to-point metric for ortogonal transformations [28]. Let's denote by $X=\{x_1,\dots,x_n\}$ the 3d data about the source RGB-D frame and by $Y=\{y_1,\dots,y_m\}$ the data about the target RGB-D frame in $\mathbb{R}^3$. Let the relationship between points in frames X and Y be such that for each point in x_i, the corresponding point in y_i can be calculated. Let S(Y) be a surface constructed from a cloud of points Y, $T(y_j)$ is the tangent plane to S(Y) at the point y_j .

Let's imagine the functional J(V,D) as a function:

$$J(V,D)=\alpha\frac{1}{W}\frac{1}{|A_f|}\sum_{i=1}^{n}w_i\left(\langle V*F_x^i-F_y^in^i\rangle\right)^2+ \\ +(1-\alpha)\frac{1}{W}\frac{1}{|A_d|}\sum_{i=1}^{n}w_i(\langle D*x^i-y^in^i\rangle)^2 \quad (1)$$

where F_x^i and F_y^i are singular points; V is transformation matrices for singular points, D is rotation matrice for depth data; α,W are weighting coefficients, selected empirically, α is hyperparameter, the value equal to 0.3 is used in the work; w_i and w_i are weighting coefficients that reflect the semantic properties of objects on a 3d scene; A_f a set which contains the correspondences between features points; A_d, a set which contains the correspondences between points x_j and y_j in X and Y; n^i – Hilber normal to $T(y_j)$.

Let's denote $\eta_1=\alpha\frac{1}{W}\frac{1}{|A_f|}$ and $\eta_2=(1-\alpha)\frac{1}{W}\frac{1}{|A_d|}$, then we can present the equation (1) as

$$J(V,D)=\eta_1\sum_{i=1}^{n}w_i\left(\langle VF_x^i-F_y^in^i\rangle\right)^2+ \\ +\eta_2\sum_{i=1}^{n}w_i(\langle Dx^i-y^i,n^i\rangle)^2= \\ =\eta_1\sum_{i=1}^{n}w_i\left(\langle VF_x^i,n^i\rangle\langle F_y^i,n^i\rangle\right)^2+ \\ +\eta_2\sum_{i=1}^{n}w_i(\langle Dx^i,n^i\rangle-\langle y^i,n^i\rangle)^2= \\ =\eta_1\sum_{i=1}^{n}(\langle VF_x^i,n^i\rangle)^2-2\langle VF_x^i,n^i\rangle\langle F_y^i,n^i\rangle+\left(\langle F_y^i,n^i\rangle\right)^2 \\ +\eta_2\sum_{i=1}^{n}(\langle Dx^i,n^i\rangle)^2-2\langle Dx^i,n^i\rangle\langle y^i,n^i\rangle+(\langle y^i,n^i\rangle)^2 \quad (2)$$

$\langle F_y^i,n^i\rangle$ = const and $\langle y^i,n^i\rangle$=const relative to V and D respectively, so

$$\eta_1\sum_{i=1}^{n}(\langle VF_x^i,n^i\rangle)^2-2\langle VF_x^i,n^i\rangle\langle F_y^i,n^i\rangle+ \\ +\eta_2\sum_{i=1}^{n}(\langle Dx^i,n^i\rangle)^2-2\langle Dx^i,n^i\rangle\langle y^i,n^i\rangle\longrightarrow\underset{V,D}{min} \quad (3)$$

Next, let us denote by (XN) and (FXN) the following matrices, respectively:

$$(XN)^i=x^in^i\,, \quad (4)$$

$$(FXN)^i=F_x^in^i \quad (5)$$

Notice, that:

$$\langle VF_x^i,n^i\rangle=tr(V\cdot(FXN)^i), \quad (6)$$

$$\langle Dx^i,n^i\rangle=tr(D\cdot(XN)^i). \quad (7)$$

where Tr is the trace of the matrix.

Thefore, we can rewrite equation (3) as

$$\sum_{i=1}^{n}tr\left(D\cdot\left(n_jXN\right)^i\right)=tr\left(D\left(\sum_{i=1}^{n}\left(n_jXN\right)^i\right)\right)=\alpha_j \quad (8)$$

$$\sum_{i=1}^{n} tr\left(V \cdot \left(n_j FXN\right)^i\right) = tr\left(V\left(\sum_{i=1}^{n}\left(n_j FXN\right)^i\right)\right) = \beta_j \quad (9)$$

Next, let us denote by ($n_j XN$) and ($n_j FXN$) the following matrices, respectively:

$$\left(n_j XN\right)^i = n_j^i (XN)^i \quad (10)$$

$$\left(n_j FXN\right)^i = n_j^i (FXN)^i \quad (11)$$

Notice, that:

$$n_j^i tr(D \cdot (XN)^i) = tr\left(D \cdot \left(n_j XN\right)^i\right) \quad (12)$$

$$n_j^i tr(V \cdot (FXN)^i) = tr\left(V \cdot \left(n_j FXN\right)^i\right). \quad (13)$$

Let's denote by SV^j и SD^j j = 1,2,3 the following matrices

$$\sum_{i=1}^{n}\left(n_j XN\right)^i = SD^j, \sum_{i=1}^{n}\left(n_j FXN\right)^i = SV^j \quad (14)$$

Using definitions (14), we rewrite equations (8) and (9) as

$$tr(D \cdot SD^j) = \alpha_j \quad tr(V \cdot SV^j) = \beta_j \quad (15)$$

Then we find the partial derivatives of the functional J(RD) with respect to $r_{ij}, f_{ij}, i, j = 1,2,3$

$$\sum_{k=1}^{n}\langle Dx^k, n^k\rangle x_j^k n_i^k - \sum_{k=1}^{n} x_j^k n_i^k \langle y^k, n^k\rangle = 0 \quad (16)$$

$$\sum_{k=1}^{n}\langle VF_x^k, n^k\rangle F_{jx}^k n_i^k - \sum_{k=1}^{n} F_{jx}^k n_i^k \langle F_y^k, n^k\rangle = 0 \quad (17)$$

$\sum_{i=1}^{n} F_{jx}^k n_i^k \langle F_y^k, n^k\rangle =$ const and $\sum_{k=1}^{n} x_j^k n_i^k \langle y^k, n^k\rangle =$ const relative to V and D respectively, so

$$\sum_{k=1}^{n} x_j^k n_i^k tr(D \cdot (XN)^k) = \alpha_{ij} \quad (18)$$

$$\sum_{k=1}^{n} F_{jx}^k n_i^k tr(V \cdot (FXN)^k) = \beta_{ij} \quad (19)$$

Next, let us denote by ($x_j^k n_i^k XN^k$) and ($F_{jx}^k n_i^k FXN^k$) the following matrices, respectively:

$$\sum_{k=1}^{n} tr\left(D \cdot x_j^k n_i^k XN^k\right) = \alpha_{ij} \quad (20)$$

$$\sum_{k=1}^{n} tr\left(V \cdot F_{jx}^k n_i^k FXN^k\right) = \beta_{ij} \quad (21)$$

Let's denote by SV^{ij} and SD^{ij} j = 1,2,3 the following matrices

$$\sum_{k=1}^{n} x_j^k n_i^k XN^k = SD^{ij} \text{ and } \sum_{k=1}^{n} F_j^k n_i^k FXN^k = SV^{ij} \quad (22)$$

Using definitions (22), we rewrite equations (20) and (21) as

$$\sum_{k=1}^{n} tr\,(D \cdot SD^{ij}) = \alpha_{ij} \quad (23)$$

$$\sum_{k=1}^{n} tr\,(V \cdot SV^{ij}) = \beta_{ij} \quad (24)$$

Then a set of 24 linear equations of the form can be obtained with respect to 24 variables r_{ij}, f_{ij}, t_k, b_k, i, j, k = 1, … ,3:

$$\begin{cases} tr(D \cdot SD^j) = \alpha_j \\ tr(V \cdot SV^j) = \beta_j \\ \sum_{k=1}^{n} tr\,(D \cdot SD^{ij}) = \alpha_{ij} \\ \sum_{k=1}^{n} tr\,(V \cdot SV^{ij}) = \beta_{ij} \end{cases} \quad (25)$$

III. An Accurated Fusion ICP Algorithm for Ortogonal Transformation

The ICP method that uses the point-to-plane error metric for orthogonal transformations can be presented in the form of the following iterative procedure [27]:

- Downsampling of the point cloud: preprocessing of data in one or both dense clouds of X and Y points in order to reduce the number of points in the analyzed data.
- Point matching: establishing a correspondence between two points sets (X and Y). A k-d tree is used to determine the corresponding points.
- Weighing of points pairs based on a strategy of assigning constant weights. In this paper a weight vector has been learned uising adaptive neighbors assigning process.
- Eliminating outliers in the data (RANSAC method or analogue).
- Selecting a classification quality metric for corresponding point pairs. In this paper we use the point-plane metric.
- Projection of a variety's element of linear transformation matrices onto a subvariety of orthogonal matrices.
- Key stage of the ICP algorithm: finding a solution to the variational problem using the metric chosen in step 5.

Similar to the F-ICP registration problem for affine transformations [29, 30], we will look for a joint solution to the variational problem for orthogonal transformations for the special case when V=D=RT. Let T_{km} be the geometric transformation value of the ICP algorithm based on the estimate obtained using the kinematic model of the sensor motion; k_{max} – stopping factor based on the maximum algorithm iterations number; ε – stopping factor based on the value of the minimization error E; RT* – the best (from the point of view of minimizing the distance) ortogonal transformation for the i-th step; δ – threshold value for inline points. T_{km} is used as the initial geometric transformation value if there is not enough feature point information in the RGB-D frames in the images to obtain the appropriate geometric transformation.

The detailed description of this algorithm consist of the following stages:

Step 1. Compute histograms of directional gradients using the DL GNG descriptor for images in RGB-D frames.

Step 2. Perform a data matching algorithm based on DL GNG for a pair of sequential images containing sets of singular points F_x^i and F_y^i. Obtain a solution to the variational problem of data registration for singular points using the point-plane metric in the form of a geometric transformation RT* and a set of singular points connections A_f.

Step 3. Check the condition: If $|A_f| < \delta$, то $RT^* = T_{km}$ и $A_f = \emptyset$. Let's put i=1.

Step 4. Determine the corresponding points A_d in the source and target point clouds using the kNN method. In this work we use the value k-5.

Obtain the values of the weighting coefficients for each pair A_f. The weight value is set based on the results of semantic marking of images in RGB-D frames. If a certain object in the 3d scene hasn't been assigned to one of the classes, then its default weight is set to that of the background object.

Step 5. Consider the gradient components with respect to the variables t and b (translation vectors) and и r_{ij}, f_{ij} (rotation matrices), respectively. Let us obtain the projection of an element of the variety of linear transformation matrices onto the subvariety of orthogonal matrices $F_{jx}^k n_i^k FXN^k$, $x_j^k n_i^k XN^k$ и $n_j^i XN, n_j^i FXN$.

Step 6. Solve a fusion variational problem using point-plane metric for a group of orthogonal transformations with respect to the transformation RT*, a set of connections between singular points A_f, a set of connections between points in two points clouds A_d.

Step 7. Check the condition: $(E(RT^*_i) - E(RT^*_{i+1}) < \varepsilon)$ or (Iteration number > k_{max}). If the condition is not true, then you need to return to Step 4 and increase the iteration number value i=i+1. The geometric transformation obtained at this stage is saved to verify condition (7) at the next step. If the condition is true, then the final solution of the variational problem (RT* transformation) is obtained and iterations of the method are stopped.

The iterative procedure will finish when the error $E(RT^*_i)$ E(RT*i) no longer decreases significantly or the maximum iterations has been reached. Otherwise, the fusion variational problem ICP is solved with respect to the most recent transformation. Step 5 has a high computational complexity, so in the general case solving the fusion ICP problem for affine transformations is a less expensive procedure then for ortogonal transformations.

IV. Computer Simulation

In this section, the results of computer sumulation are presented and discussed. For computer simulation with a graphics processor based on Intel Core i7 was used. For tests we used a data collection of archaeological monuments in the Chelyabinsk region. This data collection was compiled for archaeological sites of the Bronze Age of the Southern Trans-Urals [31]. The data sample contains: 2D data based on a collection of aerial photographs and Earth remote sensing data from the Sentinel-2, Landsat 4-9, Resurs-P, Kanopus-V satellites and 3d data in the form of tacheometric survey results, LiDAR depth scanners in the form of orthophotos and point clouds, as well as electrical survey results. The example 3d model in form of tacheometric survey results for village Stepnoe was presented on Fig. 1, example of 2D data in form of aerial photograph for village Stepnoe was presented on Fig. 2.

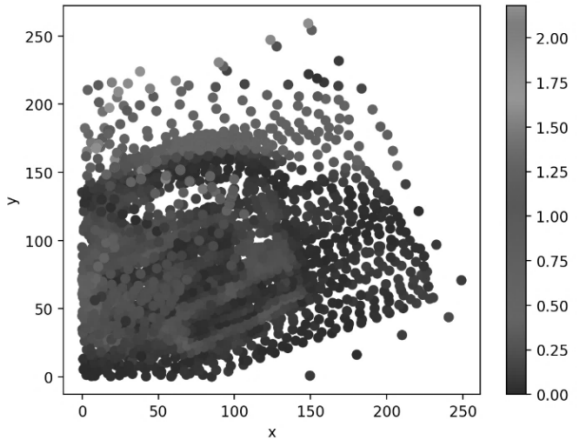

Fig. 1. Tacheometric survey results for village Stepnoe.

The signs of deciphering archaeological objects characteristic of Bronze Age monuments of the Southern Trans-Urals were defined based on the Archaeological Atlas of the Chelyabinsk Region (Kizilsky district), created by prof. Zdanovich G.B [31].

Fig. 2. Aerial photographs for village Stepnoe.

Let's evaluate the accuracy and convergence of the proposed method using the example of an annotated collection of digital data on archaeological monuments of the Bronze Age of the Southern Trans-Urals. In this paper the study of the accuracy and convergence of the proposed Fusion-ICP method for registering 3d data and state-of the art methods for registering 3d data based on the ICP method was conducted. Methods for solving the variational ICP problem were considered using various options for minimizing the functional: Horn's method based on point-to-plane using Unit Quaternions [32], Horn's method based on point-to-plane with Orthonormal Matrices extrapolation [33]. To conduct a comparative analysis of ICP registration methods in terms of accuracy, the root mean square error (RMSE) was used. Computer simulations were carried out controlled conditions (Fig.3) and under with

uncontrolled conditions in the presence of noise from matrix receivers (Fig.4).

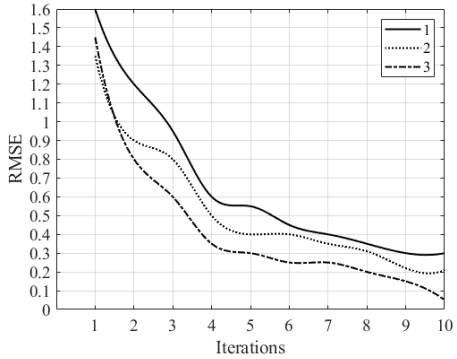

Fig. 3. Comparative analysis of registration methods in terms of convergence in controlled conditions (1- point-to-plane using Unit Quaternions; 2- point-to-plane with Orthonormal Matrices extrapolation; 3- algorithm F-ICP).

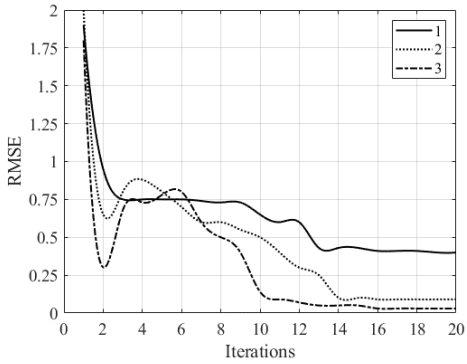

Fig. 4. Comparative analysis of registration methods in terms of convergence in uncontrolled conditions (1- point-to-plane using Unit Quaternions; 2- point-to-plane with Orthonormal Matrices extrapolation; 3 - algorithm F-ICP).

The computational experiments have shown a significant increase in the accuracy of the F-ICP algorithm in controlled conditions. The F-ICP algorithm improves the quality of the work of two key steps of the ICP algorithm determining the corresponding points between a pair of point clouds and solving the variational problem and differs from the state of art methods in that:

- F-ICP algorithm allow solving the problem of the dependence of the result of solving the variational problem ICP on the correctness of the choice of initial values;
- F-ICP algorithm is used to register point clouds with arbitrary spatial resolution and scale relative to each other;
- F-ICP algorithm accurate estimates for complex large-scale archaeological sites.

Under controlled conditions the F-ICP algorithm for registering point clouds has a convergence plot like to the convergence plot of the ICP algorithm using the point-to-point metric with extrapolation and under uncontrolled conditions the F-ICP algotithm converges 2 iterations later than the above data recording algorithms (Fig. 4), but at the same time shows better accuracy.

Figure 5 shows the result of reconstruction in the form of a dense point cloud of an archaeological site in the area of the Stepnoye settlement using the proposed 3d data registration method. Figure 6 shows the result of decoding of the archaeological monument Stepnoye in the form settlement scheme.

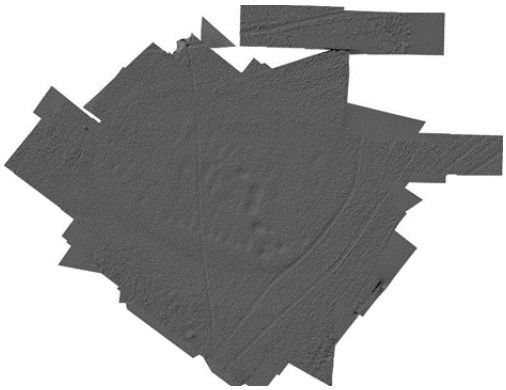

Fig. 5. Result of reconstruction of an archaeological site in the area of the Stepenoye.

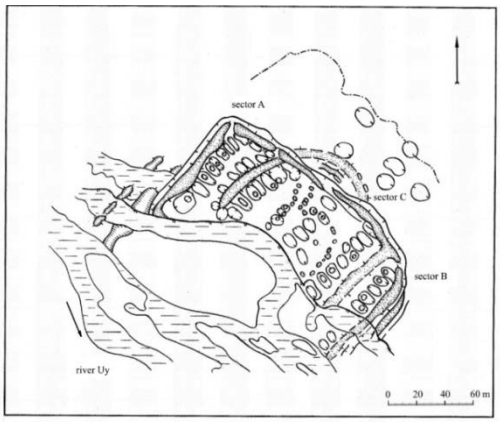

Fig. 6. The Stepnoye settlement scheme.

V. CONCLUSIONS

The paper presents the Fusion-ICP data registration algorithm using ortogonal transformations for reconstructing 3d models of an archaeological sites. The paper proposes an accurate Fusion Iterative Closest Points algorithm (F-ICP) for registering for a group of ortogonal transformations to allow the reconstruction of an archaeological objects in the form of point cloud based on solving the ICP variational problem in a closed form using the point-to-plane metric. The proposed F-ICP algorithm improves the quality of the work of two key steps of the ICP method: determining the corresponding points between a pair of point clouds and solving the variational problem. F-ICP algorithm accurate estimates for complex large-scale archaeological sites. The development of an information system for remote technology of non-destructive archaeological research allows, on the one hand, to solve the most important problem of archaeological science, related to the preservation of cultural heritage, and to increase the efficiency of identifying and protecting archaeological sites, and on the other hand, to reduce the duration of the archaeological examination procedure and to proceed to the

soonest involvement of the southern part of the Chelyabinsk region in agricultural turnover and industrial development. The system will allow monitoring the changes of the state of archaeological sites in dynamics and fix signs of destruction based on satellite imagery data.

ACKNOWLEDGMENT

The work was supported by the Russian Science Foundation and Chelyabinsk Region, project no. 23-11-20007.

REFERENCES

[1] K. Lambers, W.V. der Vaart, and Q. P. G. Bourgeois, "Integrating remote sensing, machine learning, and citizen science in dutch archaeological prospection," Remote Sensing, vol. 11 (7), pp. 794, March 2019, doi: 10.3390/rs11070794.

[2] A. Bonhage, M. Eltaher, T. Raab, M. Breuß, A. Raab, and A. Schneider, "A modified mask region-based convolutional neural network approach for the automated detection of archaeological sites on high-resolution light detection and ranging-derived digital elevation models in the North German Lowland," Archaeological Prospection, vol. 28 (2), pp. 177–186, February 2021, doi: 10.1002/arp.1806.

[3] D. S. Davis, G. Caspari, C. P. Lipo, and M. C. Sanger, "Deep learning reveals extent of Archaic Native American shell-ring building practices," J. Archaeol. Sci., vol. 132, pp. 105433, July 2021.

[4] D. S. Davis and J. Lundin, "Locating charcoal production sites in sweden using LiDAR, hydrological algorithms, and deep learning," Remote Sensing, vol. 13 (18), pp. 3680, September 2021.

[5] Ø. D. Trier, D. C. Cowley, and A. U. Waldeland," Using deep neural networks on airborne laser scanning data: Results from a case study of semi-automatic mapping of archaeological topography on Arran Scotland," Archaeological Prospection, vol. 26 (272), pp. 165–175, November 2018, doi: 10.1002/arp.1731.

[6] S. Horna, D. Meneveaux, G. Damiand, and Y. Bertrand , "Consistency constraints and 3D building reconstruction," Computer Aided Design and Application. vol. 41(1), pp. 13–27, January 2009.

[7] S. Lee, D. Feng, C. Grimm, and B. Gooch, "A sketch-based user interface for reconstructing architectural drawings," Computer Graphics Forum, vol. 27(1), pp. 81–90, March 2008.

[8] T. Li, B. Shu, X. Qiu, and Z. Wang, "Efficient reconstruction from architectural drawings," International Journal of Computer Applications in Technology, vol. 38. (1-3), pp. 177–184, July 2010.

[9] H. Edelsbrunner, "Alpha shapes—A survey," Tessellations Sci., vol. 27, pp. 1–25, January 2010.

[10] X. Ning, J. Ma, Z. Lv, Q. Xu, and Y. Wang, "Structure reconstruction of indoor scene from terrestrial laser scanner," in E-Learning and Games. Eds. New York:Springer Publishing, 2019, pp. 91–98.

[11] M. Previtali, L. Díaz-Vilariño, and M. Scaioni, "Indoor building reconstruction from occluded point clouds using graph-cut and ray-tracing," Applied Sciences, vol. 8 (9), pp. 1529, September 2018.

[12] Z. Kang, R. Zhong, A. Wu, Z. Shi, and Z. Luo, "An efficient planar feature fitting method using point cloud simplification and threshold-independent BaySAC," IEEE Geoscience and Remote Sensing Letters. vol. 13(12), pp. 1842–1846, Nov. 2016.

[13] R. Wang, L. Xie, and D. Chen, "Modeling indoor spaces using decomposition and reconstruction of structural elements," Photogrammetric Engineering & Remote Sensing, vol. 83(12), pp. 827–841, December 2017, doi: 10.14358/PERS.83.12.827.

[14] N. Silberman and R. Fergus, "Indoor scene segmentation using a structured light sensor," IEEE Proceedings of International Conference on Computer Vision Workshops (ICCV Workshops), Spain, vol. 1. pp. 601–608, November 2011.

[15] X. Ren, L. Bo, and D. Fox, "Rgb-(d) scene labeling: Features and algorithms," IEEE Proceedings of Conference on Computer Vision and Pattern Recognition, USA, vol. 1. pp. 2759–2766, June 2012.

[16] S. Gupta, P. Arbelaez, and J. Malik, "Perceptual organization and recognition of indoor scenes from RGB-D images," IEEE Proceedings of the Conference on Computer Vision and Pattern Recognition, USA, vol. 1, pp. 564–571, June 2013.

[17] R. Girshick, J. Donahue, T. Darrell, and J. Malik, "Rich feature hierarchies for accurate object detection and semantic segmentation," IEEE Proceedings of the Conference on Computer Vision and Pattern Recognition, Columbus, USA, vol. 1. pp. 580–587, June 2014.

[18] L.-C. Chen, G. Papandreou, I. Kokkinos, K. Murphy, and A. L. Yuille, "Semantic image segmentation with deep convolutional nets and fully connected." [Online]. Available: arXiv:1412.7062 [crfs], (access date: 2023/01/09).

[19] J. Long, E. Shelhamer, and T. Darrell, "Fully convolutional networks for semantic segmentation," IEEE Proceedings of the Conference on Computer Vision and Pattern Recognition, USA, pp. 3431–3440, June 2015.

[20] H. Tran, K. Khoshelham, A. Kealy, and L. Díaz-Vilariño, "Extracting topological relations between indoor spaces from point clouds," ISPRS Ann. Photogramm. Remote Sens. Spat. Inf. Sci., IV-2/W4, pp. 401–406, September 2017, doi: 10.5194/isprs-annals-IV-2-W4-401-2017.

[21] S.Thrun and A. Bücken, "Integrating grid-based and topological maps for mobile robot navigation," Proceedings of the National Conference on Artificial Intelligence, USA, vol. 1, pp. 4–6, August 1996.

[22] K. Joo, T.-K. Lee, S. Baek, and S.-Y. Oh, "Generating topological map from occupancy grid-map using virtual door detection," IEEE Proceedings of the Congress on Evolutionary Computation, Spain, vol. 1, pp. 1–6, July 2010.

[23] D. Gonzalez-Arjona, A.Sanchez, F. López-Colino, A. De Castro, and J. Garrido, "Simplified occupancy grid indoor mapping optimized for low-cost robots," ISPRS Journal of Photogrammetry and Remote Sensing, vol. 2(4), pp. 959–977, October 2013, doi: 10.3390/ijgi2040959.

[24] D. Demyen and M. Buro, "Efficient triangulation-based pathfinding," Proceedings of the AAAI Conference on Artificial Intelligence," USA, vol. 21, pp. 942–947, July 2006.

[25] A. Kontarinis, K. Zeitouni, C. Marinica, D. Vodislav, and D. Kotzinos, "Towards a semantic indoor trajectory model," Proceedings of the 2nd International Workshop on "Big Mobility Data Analytics" (BMDA) with EDBT, Portugal, vol. 1, pp. 1–9, March 2019.

[26] P. Besl and N. McKay, "A method for registration of 3-D shapes," IEEE Transactions on Pattern Analysis and Machine Intelligence, 1992, vol. 14(2), pp. 239–256, March 2019, doi: 10.1109/34.121791.

[27] S. Rusinkiewicz and M. Levoy, "Efficient variants of the ICP algorithm," IEEE Proceedings of International Conference on 3-D Digital Imaging and Modeling (3DIM), Canada, vol. 1, pp.145–152, May-June 2001.

[28] A. V. Vokhmintcev, A. V. Melnikov, K. V. Mironov, and V. V. Burlutskiy, "Reconstruction of three-dimensional map based on closed form solution of variational problem of multi- sensor data registration," Doklady Mathematics, vol. 99(1), pp. 108–112, May 2019.

[29] A. V. Vokhmintcev, A. V. Melnikov, and S. A. Pachganov, "Simultaneous localization and mapping method in three-dimensional space based on the combined solution of the point-point variation problem icp for an affine transformation," Informatics and Applications, vol. 14(1), pp. 101–112, 2020, doi: 10.14357/19922264200114.

[30] A. Vokhmintcev and M. Timchenko, "The new combined method of the generation of a 3d dense map of environment based on history of camera positions and the robot's movements," Acta Polytechnica Hungarica, vol. 17(8), pp. 95–108, January 2020, doi: 10.12700/APH.17.8.2020.8.7.

[31] G. B. Zdanovich, I. M. Batanina, N. V. Levit, and S. A. Batanin, "Steppe–forest-steppe. Kizilsky district. Archaeological atlas of the Chelyabinsk region." [Online]. Available: https://search.rsl.ru/ru/record/01002755616?ysclid=lm3sa1zfkp696194850 (access date: 2023/01/09).

[32] B. Horn, "Closed-form solution of absolute orientation using unit quaternions," Journal of the Optical Society of America. A, vol. 4(4), pp. 629–642, April 1987, doi: 10.1364/JOSAA.4.000629.

[33] B. Horn, H. Hilden, and S. Negahdaripour, "Closed-form solution of absolute orientation using orthonormal matrices," Journal of the Optical Society of America A, vol. 5(7), pp. 1127–1135, July 1988, doi: 10.1364/JOSAA.5.001127.